LANGMUIR

Article

pubs.acs.org/Langmuir

Immobilization Strategies for Functional Complement Convertase Assembly at Lipid Membrane Interfaces

Saziye Yorulmaz Avsar,[†,‡,§] Joshua A. Jackman,[†,‡] Min Chul Kim,[†,‡] Bo Kyeong Yoon,[†,‡] Walter Hunziker,[§,∥,⊥] and Nam-Joon Cho*[,†,‡,#]

[†]School of Materials Science and Engineering, Nanyang Technological University, 50 Nanyang Avenue, Singapore 639798 Singapore

[‡]Centre for Biomimetic Sensor Science, Nanyang Technological University, 50 Nanyang Drive, Singapore 637553, Singapore

[§]Institute of Molecular and Cell Biology, Agency for Science Technology and Research, Singapore 138673, Singapore

[∥]Department of Physiology, Yong Loo Lin School of Medicine, National University of Singapore, Singapore 117599, Singapore

[⊥]Singapore Eye Research Institute, Singapore 169856, Singapore

[#]School of Chemical and Biomedical Engineering, Nanyang Technological University, 62 Nanyang Drive, Singapore 637459, Singapore

Supporting Information

ABSTRACT: The self-assembly formation of complement convertases—essential biomacromolecular complexes that amplify innate immune responses—is triggered by protein adsorption. Herein, a supported lipid bilayer platform was utilized to investigate the effects of covalent and noncovalent tethering strategies on the self-assembly of alternative pathway C3 convertase components, starting with C3b protein adsorption followed bythe addition of factors B and D. Quartz crystal microbalance-dissipation (QCM-D) experiments measured the real-time kinetics of convertase assembly onto supported lipid bilayers. The results demonstrate that the nature of C3b immobilization onto supported lipid bilayers is a key factor governing convertase assembly. The covalent attachment of C3b to maleimide-functionalized supported lipid bilayers promoted the self-assembly of functional C3 convertase in the membrane-associated state and further enabled successful evaluation of a clinically relevant complement inhibitor, compstatin. By contrast, noncovalent attachment of C3b to negatively charged supported lipid bilayers also permitted C3b protein uptake, albeit membrane-associated C3b did not support convertase assembly in this case. Taken together, the findings in this work demonstrate that the attachment scheme for immobilizing C3b protein at lipid membrane interfaces is critical for downstream C3 convertase assembly, thereby offering guidance for the design and evaluation of membrane-associated biomacromolecular complexes.

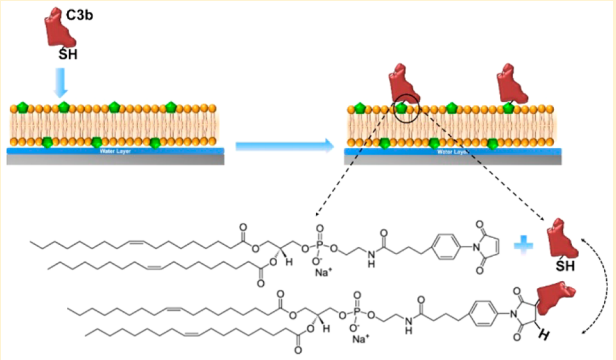

INTRODUCTION

The complement system is a key part of the innate immune response that defends against pathogenic entities such as microbes, apoptotic cells, and immune complexes.[1,2] A combination of soluble and membrane-bound complement proteins act synergistically in order to eliminate invading entities by either labeling them for phagocytosis or producing anaphylatoxins (chemoattractants) to recruit immune cells.[3] Furthermore, complement proteins are able to directly kill invading entities, particularly lipid-membrane-enclosed particulates (e.g., bacteria) through the assembly of a pore-forming membrane attack complex (MAC).[3] Collectively, all of these effector responses are known as complement activation, and there is a delicate balance of regulatory factors that manage basal complement levels because effector molecules such as anaphylatoxins and MAC complexes can act indiscriminately.[4,5] Indeed, if complement activation is not tightly controlled, the generation of excessive quantities of effector molecules may lead to an immune imbalance, resulting in complement-mediated disorders (autoimmune diseases) or serious tissue damage associated with unregulated complement attack on themselves.[6,7]

Complement proteins are normally inactive in blood circulation and become active only once they interact with pathogenic entities. Indeed, protein adsorption onto target surfaces initiates complement activation, and the specific complement proteins involved in the adsorption process dictate the complement response through either the classical, lectin, or alternative pathway.[8−10] The classical pathway is triggered by C1q protein binding, and the lectin pathway is activated by the

Received: May 1, 2017
Revised: June 22, 2017
Published: July 6, 2017

DOI: 10.1021/acs.langmuir.7b01465
Langmuir 2017, 33, 7332−7342

Table 1. Characteristics and Functional Roles of Complement Proteins Involved in the Formation of Alternative Pathway Convertases

protein	molecular weight (kDa)	serum concentration (μg/mL)	isoelectric point	key function(s)
C3	185	1200−1500	5.9	responsible for amplification of complement activation through the generation of active C3b
C3b	176	N/A	5.7	an opsonin as well as a structural component of complement convertases
iC3b	176	N/A	5.7	inactivated form of C3b
factor B	93	200−210	5.6−6.1	catalytic subunit of C3 alternative pathway convertase
factor D	24	1−2	7.4	cleaves factor B, which becomes bound to C3b

attachment of mannan-binding lectin. On the other hand, the alternative pathway is initiated by the spontaneous hydrolysis of C3 in the solution phase or the adsorption of one or more recognition molecules, namely, C3, C3b, and properdin. After initiation, all three pathways converge, leading to the formation of a surface-bound enzymatic complex, most prominently the C3 convertase that catalyzes the cleavage of complement C3 protein in the blood. This proteolytic event generates two different protein fragments, C3a and C3b. The smaller fragment, C3a, is an anaphylatoxin that induces inflammation and is also used as a biomarker of complement activation. On the other hand, the larger fragment, C3b, is a biologically active fragment that covalently attaches to free hydroxyl or amino groups that are present on target-surface-presenting proteins and carbohydrates via covalent ester or amide bonds, respectively, thereby stimulating phagocytosis or MAC-induced cytolysis.[11] Moreover, surface-adsorbed C3b provides binding sites for factor B and other complement proteins such as regulatory complement factor H.[12,13] The binding of factor B leads to the formation of a C3bB proconvertase, and this macromolecular complex is subsequently cleaved by factor D in order to yield an alternative pathway C3 convertase, C3bBb, which in turn promotes the generation of more C3b proteins.[14,15] As a result, the close relationship between C3 convertase assembly and C3b generation instigates a positive feedback loop that amplifies the total complement activation independently of which pathway was initially triggered.[2,8,16,17] However, when attached C3b is associated with factor H instead of factor B, the alternative pathway convertase is no longer assembled.[18−20] Hence, the self-assembly of functional convertases is regulated and involves a highly orchestrated sequence of protein−surface and protein−protein interactions.

To probe the stepwise assembly of alternative pathway convertases on model surfaces, surface-sensitive measurement approaches have proven useful. Nilsson et al. first conducted surface plasmon resonance (SPR) experiments in order to monitor convertase assembly as well as drug-mediated inhibition (i.e., compstatin peptide) of complement activation.[21] Of note, in that study, the convertase initiator, C3b, was covalently attached to the carboxymethyl dextran-coated sensor surface through amine coupling. Using similar covalent attachment schemes, the effects of other complement regulatory proteins such as the decay-accelerating factor (DAF, CD55) and properdin (factor P) on convertase assembly and complement activation have also been investigated.[22,23] In later studies, different C3b immobilization schemes—covalent amine coupling or activated hydroxyl coupling—were compared, revealing that the type of immobilization affects C3b conformation although both conformations facilitated convertase assembly.[24,25] Although oriented C3b immobilization schemes support in situ convertase assembly, there are technical challenges such as the high degrees of nonspecific protein adsorption when using conventional carboxymethyl dextran surfaces.[26] In an alternative approach, Sarrias et al. demonstrated the attachment of biotinylated C3b onto streptavidin-coated surfaces in an oriented manner,[27] enabling the investigation of alternative pathway C5 convertases.[28] Furthermore, on polystyrene surfaces, quartz crystal microbalance-dissipation (QCM-D) measurements have detected convertase assembly arising from noncovalent C3b adsorption.[29] Accordingly, there is debate about the importance of the attachment scheme—covalent versus noncovalent coupling—between the C3b protein and the target surface.[30]

Such questions become particularly important when considering that existing convertase assembly studies have focused on interactions occurring on synthetic biomaterial surfaces with fouling properties, characteristics that contrast starkly with those of biological interfaces such as nonfouling lipid membranes. Toward this goal, artificial membrane platforms such as supported lipid bilayer (SLB) platforms are widely utilized for immunological studies and are an ideal choice for studying convertase assembly in the context of biological membranes.[31,32] SLBs can be investigated using a wide range of surface-sensitive measurement techniques, and their lipid composition is tunable in order to control parameters such as the membrane surface charge and functional group presentation, the latter of which facilitates biomolecule conjugation.[33] The SLB platform has facilitated mechanistic investigations into how complement inhibitors such as clusterin and vitronectin interfere with MAC assembly[34,35] as well as the membrane surface charge preferences of different complement proteins,[36] and it also presents unique opportunities for studying the function of membrane proteins in general.[37−39] Covalent immobilization of complement proteins to SLBs remains to be investigated, and identifying an optimal scheme to form convertase assemblies on lipid membranes is an outstanding goal.

The aim of the present study is to develop an experimental platform that permits the assembly and evaluation of functional convertases at lipid membrane interfaces. Noncovalent and covalent immobilization schemes were utilized in order to attach C3b protein to SLBs, followed by the addition of complement factors B and D to trigger convertase assembly. The individual steps of convertase assembly were monitored in real time by QCM-D measurements, with fluorescence microscopy employed in order to confirm the selective, covalent attachment of C3b to functionalized SLBs. The results obtained provide guidance on useful strategies for establishing complement convertases at lipid membrane interfaces toward functional evaluation and inhibitor studies.

DOI: 10.1021/acs.langmuir.7b01465
Langmuir 2017, 33, 7332−7342

MATERIALS AND METHODS

Protein Reagents. Purified human C3, C3b, iC3b, factor B, and factor D proteins were obtained from Complement Technology (Tyler, TX). FITC-labeled polyclonal C3c antibodies were obtained from Dako (Glostrup, Denmark). Compstatin was received in lyophilized powder form from Tocris (Bristol, U.K.) and directly reconstituted in the appropriate aqueous buffer solution for experiments. As presented in Table 1, C3 is the most abundant complement protein in plasma and has a molar mass of 185 kDa. C3b protein is a 176 kDa fragment of the C3 protein that is obtained through proteolytic cleavage. Both C3 and C3b proteins have isoelectric points below 6 and possess negative net charges under neutral pH conditions.[40,41] Factor B is a serine protease that interacts with surface-bound C3b and solution-phase C3(H_2O) in order to form membrane-bound C3bB and soluble C3(H_2O)B proconvertases, respectively.[42] Factor D is another serine protease that cleaves factor B when factor B is bound to C3b or C3 (H_2O).[43,44] iC3b is the inactivated form of C3b and consequently lacks binding sites for complement factors and C5. Because iC3b does not interact with factor B, membrane association of iC3b cannot trigger convertase assembly. Compstatin is a cyclic C3-binding peptide with a molecular weight of 1550.77 Da, and it has the following amino acid sequence: ICVVQDWGHHRCT-NH_2.[45] Stock aliquots of complement proteins were prepared in a 10 mM sodium phosphate [pH 7.2] buffer solution with 145 mM NaCl, and they were stored at −80 °C. The FITC-labeled antibody and compstatin were stored at −20 °C. Immediately before the experiment, the proteins were diluted to the appropriate test concentration in a 10 mM Tris [pH 7.2] buffer solution with 150 mM NaCl and 5 mM $MgCl_2$.

Lipid Reagents. 1,2-Dioleoyl-*sn*-glycero-3-phosphocholine (DOPC), 1,2-dioleoyl-*sn*-glycero-3-phosphoethanolamine-*N*-[4-(*p*-maleimidophenyl)butyramide] (sodium salt) (MPB-PE), and 1-palmitoyl-2-oleoyl-*sn*-glycero-3-phospho-(1′-*rac*-glycerol) (sodium salt) (POPG) were obtained in lyophilized powder form, and 1,2-dioleoyl-*sn*-glycero-3-phosphoethanolamine-*N*-(lissamine rhodamine B sulfonyl) (ammonium salt) (Rh-PE fluorophore) was received in chloroform from Avanti Polar Lipids (Alabaster, AL). The lipid powders were stored at −20 °C until the experiment and were then diluted in the appropriate organic solvent.

Quartz Crystal Microbalance-Dissipation (QCM-D) Monitoring. A Q-Sense E4 instrument (Biolin Scientific, Gothenburg, Sweden) was used to monitor in situ adsorption processes by tracking real-time changes in the resonance frequency and energy dissipation of a silicon oxide-coated quartz crystal sensor chip (model no. QSX303) at multiple odd overtones (n = 3, 5, and 7 overtones). Because the measurements were conducted on single-layer SLB films, it is understood that the measurement responses occur primarily via biochemical effects associated with the macromolecular interactions under consideration (e.g., protein adsorption or binding) rather than mechanical effects induced by the measurement operation itself such as those that can occur in multilayer films.[46] All reported data herein were recorded at 25 MHz (n = 5 overtone) and normalized accordingly ($\Delta f_{n=5}/5$). Before experiment, the QCM-D sensor surfaces were washed sequentially with 1 wt % sodium dodecyl sulfate, water, and ethanol, followed by drying with a gentle stream of nitrogen gas. The sensor surfaces were then exposed to oxygen plasma treatment (Harrick Plasma, Ithaca, NY) at maximum radio frequency power in order to remove any residual organic contaminants. After establishing baseline signals in aqueous buffer solution, the QCM-D measurements were conducted under continuous flow conditions, with the flow rate defined as 100 μL/min for all steps of bilayer formation and washing processes and 41.8 μL/min for protein addition steps, as controlled by a Reglo Digital peristaltic pump (Ismatec, Glattbrugg, Switzerland). The temperature of the flow cell was fixed at 24.0 ± 0.5 °C.

Epifluorescence Microscopy. Fluorescence microscopy experiments were conducted on SLBs containing 0.5 mol % Rhodamine-DHPE lipid by using an inverted epifluorescence Eclipse TI microscope (Nikon) equipped with a 60× oil-immersion objective (NA 1.49) and an Andor iXon+ EMCCD camera (Andor Technology, Belfast, Northern Ireland). The SLBs were formed in a microfluidic channel configuration (sticky-Slide IV0.4 Luer, Ibidi, Munich, Germany), and 500 nM C3b protein was injected onto SLB-coated surfaces at a flow rate of 50 μL/min for 15 min, followed by the injection of 100 μg/mL FITC-labeled C3c antibody at the same flow rate for 15 min and a subsequent buffer wash. The acquired images consisted of 512 pixels × 512 pixels, resulting in an image size of 136 μm × 136 μm. The samples were visualized using TRITC (rhodamine−DHPE lipid) and FITC (C3c antibody) filter sets with a mercury lamp (Intensilight C-HGFIE; Nikon Corporation).

Fluorescence Microscopy after Photobleaching (FRAP). A 20-μm-wide circular spot was photobleached for 5 s with a 532 nm, 100 mW laser beam, followed by time-lapse recording for a total of 2 min. Diffusion coefficients were determined on the basis of the Hankel transform method.[47] For all fluorescence microscopy imaging experiments, thin glass coverslips (Menzel Gläser, Braunschweig, Germany) were assembled with the commercially available microfluidic chambers as described above.

Supported Lipid Bilayer (SLB) Formation. The solvent-assisted lipid bilayer (SALB) formation method was employed in order to prepare SLBs. For SALB experiments, the DOPC and MPB-PE lipid powders were dissolved in isopropanol at stock concentrations of 10 and 1 mg/mL, respectively. The POPG lipid powder was dissolved in ethanol at a concentration of 5 mg/mL and incubated at 40 °C in order to promote complete lipid solubilization. Before the experiment, the lipid solutions were mixed to the desired molar ratio and diluted in isopropanol to a final concentration of 0.5 mg/mL. As part of the SALB experimental protocol, a measurement baseline was first recorded in aqueous buffer solution (10 mM Tris [pH 7.5] with 150 mM NaCl) (step 1), followed by exchange with isopropanol solution (step 2). Then, 0.5 mg/mL lipid in isopropanol was deposited onto the substrate (step 3) and incubated for approximately 10 min before a solvent-exchange step was performed as aqueous buffer solution was reintroduced, leading to bilayer formation (step 4). After bilayer formation, 0.1 mg/mL bovine serum albumin (BSA) was added (step 5) in order to verify the completeness of bilayer formation and passivate any exposed surfaces.

Liposome Preparation. Lipid powders were suspended in chloroform and then mixed to the desired molar ratio. The lipid compositions were either 100 mol % DOPC, 70/30 mol % DOPC/POPG, or 70/30 mol % DOPC/MPB-PE. In all cases, a dried lipid film was formed by evaporating the chloroform upon exposure to a gentle stream of nitrogen gas. The dried lipid films were then placed in a vacuum desiccator overnight in order to remove residual chloroform. After storage, the dried lipid films were hydrated at a concentration of 5 mg/mL in 10 mM Tris [pH 7.5] buffer solution with 150 mM NaCl and 5 mM $MgCl_2$ and subjected to vortex mixing. The resulting liposome suspensions were extruded a minimum of 13 times through a track-etched polycarbonate membrane with 200-nm-diameter pores by using a mini-extruder apparatus (Avanti Polar Lipids). The extruded liposome samples had an average diameter of around 170 nm.

Circular Dichroism (CD) Spectroscopy. UV circular dichroism spectra of C3b in the absence or presence of liposomes were obtained by using an AVIV model 420 spectrometer (AVIV Biomedical, Lakewood, NJ, USA) with a 1 mm path length cuvette (Hellma). Spectra data were collected with a step size of 0.5 nm and an averaging time of 4 s. The C3b and liposome concentrations were fixed at 2.5 μM and 1 mM, respectively, and the mixture was 10 mM Tris [pH 7.5] buffer solution with 150 mM NaCl and 5 mM $MgCl_2$ for 30 min at ambient temperature prior to the experiment. All spectra were recorded at 25 °C from 190 to 260 nm using a bandwidth of 1 nm and averaged over three scans. Baseline scans were obtained using the same parameters for buffer with liposomes only and subtracted from the respective data scans with the C3b protein. The final corrected averaged spectra are expressed in mean residue molar ellipticity, and the secondary structure characteristics of the C3b protein were analyzed using the BeStSel (β-structure selection) web server program that is available at bestsel.elte.hu.[48]

Statistical Analysis. Measurements were conducted in triplicate, and the results are expressed as the mean ± the standard deviation

DOI: 10.1021/acs.langmuir.7b01465
Langmuir 2017, 33, 7332−7342

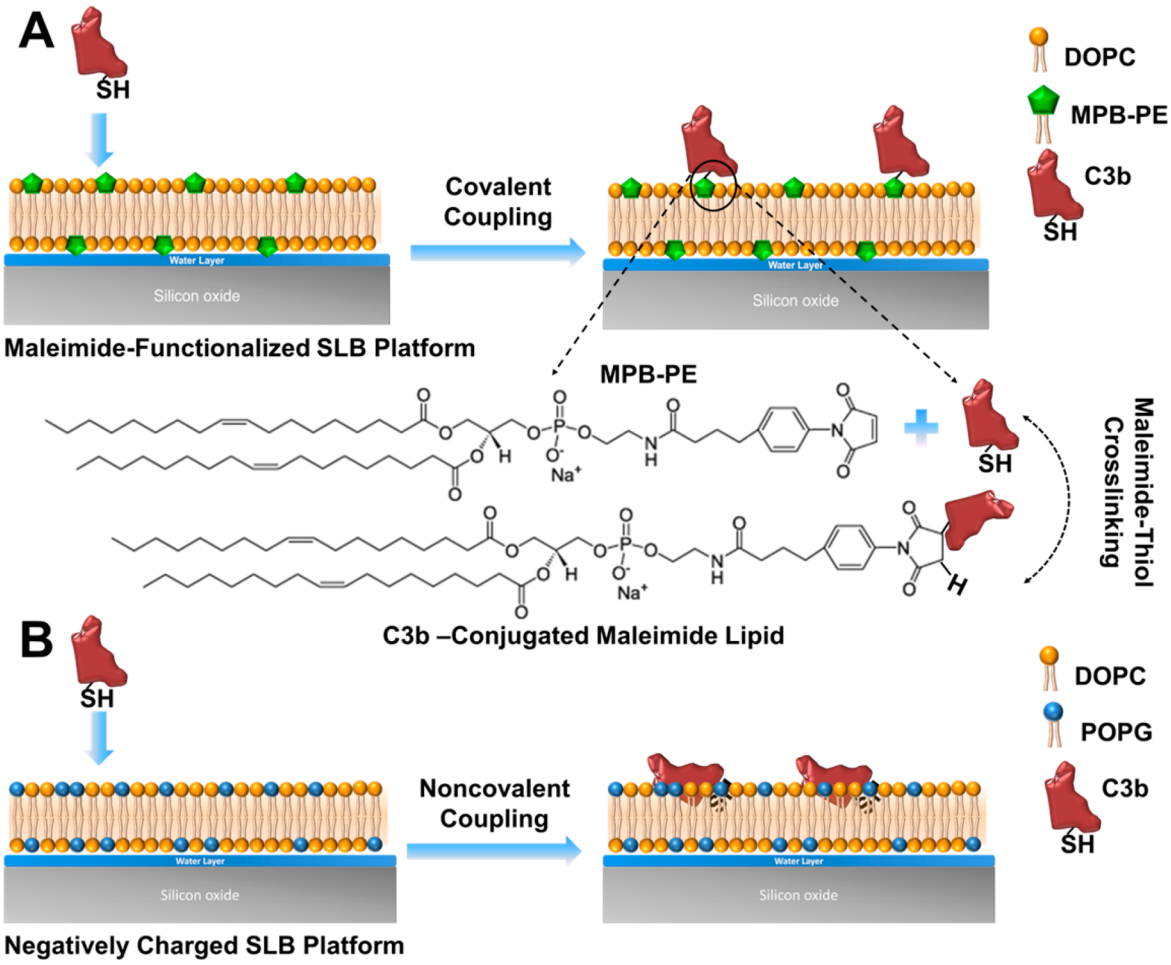

Figure 1. Schematic illustration of tethering strategies to immobilize complement C3b proteins on supported lipid bilayers. (A) Covalent attachment is achieved by employing maleimide-functionalized SLBs that become conjugated to free thiol groups on C3b proteins. (B) Noncovalent attachment is faciliated by negatively charged SLBs that promote C3b adsorption through attractive electrostatic interactions.

(SD) of the mean. Statistical analysis was performed using the OriginPro 9 software program (OriginLab Corporation, Northampton, MA). One-way analysis of variance (ANOVA) followed by the Bonferroni test was conducted, and a p value of less than 0.05 was considered to be statistically significant (*).

RESULTS

Tethering Strategies for Protein Attachment at Lipid Membrane Interfaces. Convertase assembly on the SLB platform was initiated by identifying an optimal scheme for C3b protein attachment. Two tethering strategies were employed on the basis of covalent and noncovalent conjugation, respectively (Figure 1). Both approaches began with SLB formation on silicon oxide by employing the solvent-assisted lipid bilayer (SALB) fabrication method.[49] A key advantage of the SALB method is that it enables the formation of SLBs from a wider range of lipid compositions than does the conventional vesicle fusion method. For noncovalent tethering, the chosen lipid composition was 70 mol % DOPC and 30% POPG, and it provides a negatively charged SLB that supports C3b protein adsorption, which is mediated by a positively charged domain within the C3b protein. On the other hand, for covalent tethering, a mixture of DOPC and maleimide-functionalized MPB-PE lipids was utilized for SLB preparation, with the molar fraction of the MPB-PE lipid ranging between 5 and 30 mol %. The maleimide functional group enables the formation of covalent thioether bonds between the MPB-PE lipid headgroup and the sulfhydryl groups of the C3b protein.[50]

The SLB formation process was tracked by the QCM-D measurement technique (Figure S1). Simultaneous changes in the resonance frequency (Δf) and energy dissipation (ΔD) were recorded as a function of time and reflect the mass and viscoelastic properties of the adlayer, respectively.[51] For all lipid compositions, the final QCM-D measurement responses corresponded to Δf and ΔD values of -26 ± 3 Hz and $<1 \times 10^{-6}$, respectively, which agree well with literature values for SLB systems.[49,52,53] Of note, attempts to form SLBs containing 30 mol % MPB-PE lipid were also conducted using the vesicle fusion method but did not succeed. This observation is in line with previous literature reports of SLB formation with up to 20 mol % maleimide-functionalized lipid and demonstrates the utility of the SALB method for this application.[52−54] Fluorescence recovery after photobleaching (FRAP) experiments confirmed the formation of homogeneous SLBs, and it was determined that the diffusion coefficient decreased with increasing MPB-PE lipid fraction[54] (Figure S2). Collectively, these characterization experiments validate SLB formation, thereby enabling subsequent investigation of C3b protein attachment through the different tethering strategies.

Comparison of Covalent and Noncovalent Tethering Schemes. Figure 2 presents the comparison of C3b protein attachment to SLBs. After the completion of SLB formation,

DOI: 10.1021/acs.langmuir.7b01465
Langmuir 2017, 33, 7332−7342

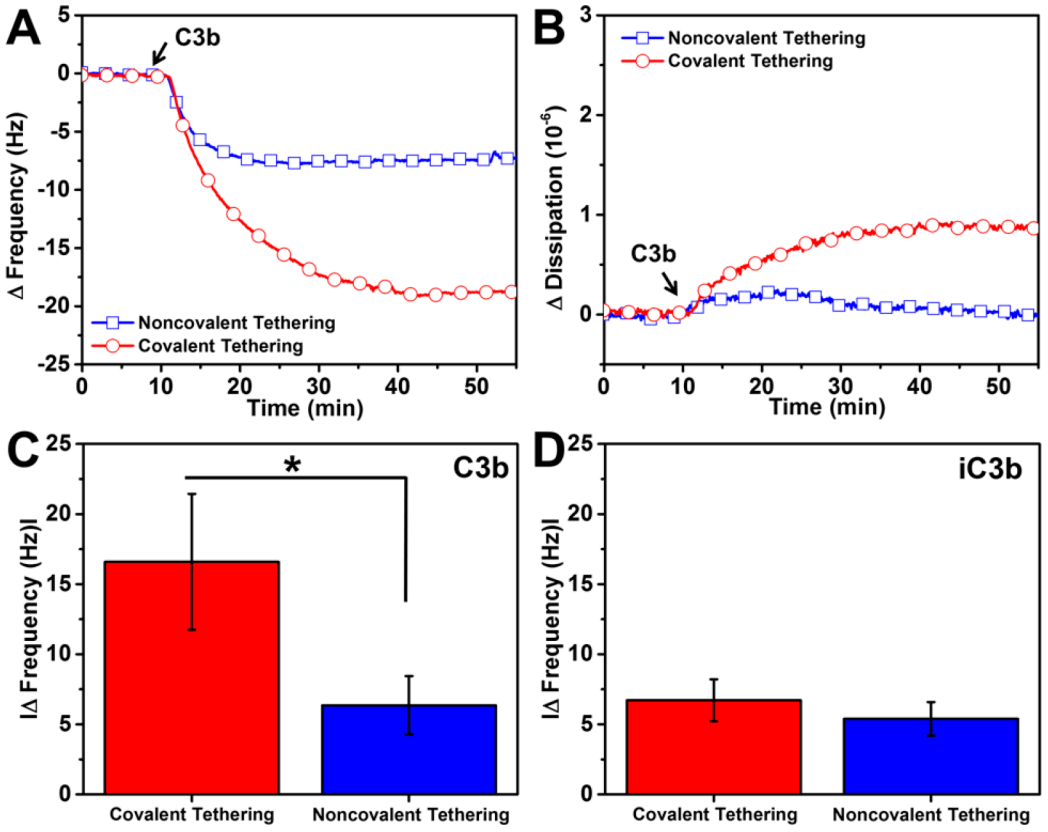

Figure 2. Comparison of covalent and noncovalent tethering strategies for C3b protein attachment. Changes in QCM-D (A) frequency and (B) energy dissipation as a function of time upon addition of C3b to SLBs (indicated by arrow) via covalent (red circles) and noncovalent (blue squares) immobilization schemes. The covalent tethering approach utilizes a 70/30 mol % DOPC/MPB-PE SLB, whereas noncovalent tethering is based on a 70/30 DOPC/POPG SLB. (C) Summary of absolute frequency shifts for C3b protein attachment to SLBs by the two different immobilization strategies. (D) Summary of absolute frequency shifts for iC3b protein attachment to SLBs by the two immobilization strategies.

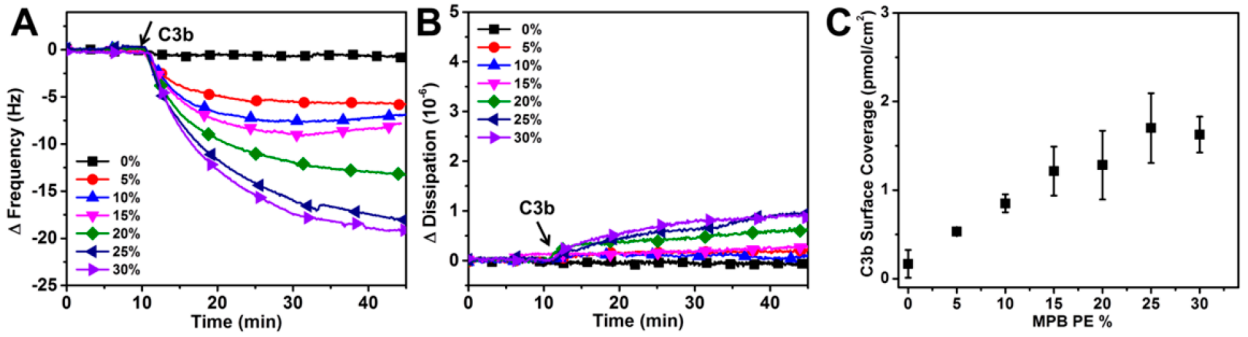

Figure 3. Controllable tethering of C3b protein to maleimide-functionalized supported lipid bilayers. Changes in the QCM-D (A) frequency and (B) energy dissipation as a function of time upon addition of C3b to functionalized SLBs (indicated by the arrow) with a variable molar percentage of MPB-PE lipid. (C) Summary of the attached C3b surface density to SLBs as a function of MPB-PE content.

the QCM-D measurement signals were normalized and the baseline signals were reestablished. After 10 min of stabilization, 500 nM C3b protein was added to negatively charged 70/30 mol % DOPC/POPG SLB (noncovalent scheme) and maleimide-functionalized 70/30 mol % DOPC/MPB-PE SLB (covalent scheme) (Figure 2A,B). C3b protein attachment to the negatively charged SLB led to a Δf shift of -6.36 ± 2.08 Hz and a negligible ΔD shift of $(0.12 \pm 0.09) \times 10^{-6}$. By contrast, appreciably more protein adsorption occurred on the maleimide-functionalized SLB with Δf and ΔD shifts of -16.59 ± 4.85 Hz and $(0.89 \pm 0.16) \times 10^{-6}$, respectively (Figure 2C). Importantly, the $\Delta f/\Delta D$ ratio provides insight into the structural properties of the attached protein, and the differences in the $\Delta f/\Delta D$ ratio for the noncovalent versus covalent tethering strategies suggest that membrane-associated C3b proteins have a different conformation in each case.[55,56]

Circular dichroism spectroscopy experiments provided corroborating evidence to support that the two immobilization schemes lead to different membrane-associated conformational states, namely, that membrane-associated C3b protein on 70/30 mol % DOPC/MPB-PE liposomes induces an appreciably greater reduction in antiparallel ß sheets as compared to membrane-associated C3b on 70/30 mol % DOPC/POPG liposomes and free C3b protein (Figure S3 and Table S1).[57]

The attachment of inactive C3b (iC3b) to the two SLB platforms was also investigated (Figure 2D). iC3b has the same

DOI: 10.1021/acs.langmuir.7b01465
Langmuir 2017, 33, 7332−7342

molecular weight and surface charge density as C3b protein, albeit with a different protein conformation that lacks both proteolytic function and binding sites for other complement proteins as well as no free sulfhydryl groups. Upon addition of 500 nM iC3b protein to the negatively charged and maleimide-functionalized SLB platforms, protein adsorption was observed, as indicated by negative Δf shifts. In both cases, the final Δf shift was around −6 Hz (Figure S4). Importantly, there was significantly more C3b attachment to maleimide-functionalized SLBs, as compared to iC3b attachment. By contrast, C3b and iC3b attachments to negatively charged SLBs were equivalent. Collectively, these findings support that the covalent attachment of C3b is driven by the formation of covalent thioether linkages, whereas electrostatic interactions result in appreciably less bound protein for the noncovalent tethering approach.

C3b Protein Conjugation to Maleimide-Functionalized SLBs. The covalent conjugation of C3b protein to maleimide-functionalized SLBs was further characterized by varying the MPB-PE molar fraction, as presented in Figure 3. C3b protein (500 nM) was added to maleimide-functionalized SLBs, and the Δf and ΔD shifts were monitored as a function of time (Figure 3A,B). Upon C3b protein adsorption, the Δf shift decreased while the ΔD shifts slightly increased. With increasing MPB-PE molar fraction in the lipid composition, the Δf shift decreased until reaching saturation of the attached protein. The ΔD shifts showed a proportional increase but always remained below 1×10^{-6}. As presented in Table 2, the

Table 2. Summary of QCM-D Frequency and Energy Dissipation Shifts for C3b Protein Attachment to Maleimide-Functionalized SLBs as a Function of the MPB-PE Molar Percentage

MPB-PE content (%)	Δfrequency (Hz)	Δenergy dissipation (10^{-6})
0	−1.67 ± 1.56	0.12 ± 0.06
5	−5.36 ± 0.42	0.11 ± 0.01
10	−8.46 ± 1.01	0.30 ± 0.24
15	−12.08 ± 2.75	0.23 ± 0.24
20	−12.76 ± 3.86	0.35 ± 0.21
25	−16.91 ± 3.92	0.78 ± 0.31
30	−16.18 ± 2.01	0.83 ± 0.15

Δf shift ranged from −5.36 ± 0.42 Hz at 5 mol % MPB-PE to −16.18 ± 2.01 Hz at 30 mol % MPE-PE. By contrast, there were negligble Δf and ΔD shifts upon C3b protein addition to 100 mol % POPC SLBs. Because of the negligible ΔD shifts in all cases, the molar surface density of attached C3b protein was estimated by the Sauerbrey relationship.[58] The surface densities varied from 0.53 ± 0.04 pmol/cm^2 at 5 mol % MPB-PE up to saturation at around 1.70 ± 0.39 pmol/cm^2 at 25 mol % MPB-PE (Figure 3C). Hence, the amount of covalently bound C3b protein was tunable on the basis of the MPB-PE molar fraction.

To determine if membrane-associated C3b protein is recognizable by conformation-specific antibodies, additional QCM-D experiments were conducted on 90/10 mol % DOPC/MPB-PE SLBs, as shown in Figure 4. In these experiments, C3b protein was added to SLBs as described above, followed by the addition of 100 μg/mL FITC-labeled C3c antibody that recognizes a fragment within the C3b protein.[29] C3b conjugation and subsequent antibody binding steps led to Δf shifts of around −8 and −43 Hz, respectively (Figure 4A). The corresponding ΔD shifts were around 0.8×10^{-6} and 5×10^{-6}, respectively. A control experiment was also performed whereby C3c antibody was directly added to the SLB in the absence of C3b protein (Figure 4B). In this case, there was no antibody binding, indicating the selective binding of C3c antibody to membrane-associated C3b. Fluorescence microscopy experiments confirmed the selective attachment of FITC-labeled C3c antibody to rhodamine-doped SLBs (Figure 4C). Although no antibody binding to the SLB was observed without membrane-associated C3b, a marked increase in the fluorescence intensity was observed when antibody was added to the C3b-coated SLB. Similar experiments were performed in the case of noncovalently tethered C3b protein on a 70/30 mol % DOPC/POPG SLB, and there was a similar amount of bound antibody in this case (Figure S5). Collectively, the results suggest that membrane-associated C3b proteins retain a functionally active orientation that may be suitable for convertase assembly.

Convertase Assembly and Functional Evaluation. We next explored the stepwise assembly of the alternative pathway C3 convertase on the SLB platforms, which was achieved by the sequential addition of C3b, a mixture of factor B and factor D, and C3 protein as presented in Figure 5A. Both covalent and noncovalent immobilization of C3b protein on the SLB were tested. The lipid compositions for all of the following experiments were either 70/30 mol % DOPC/MPB-PE (covalent scheme) or 70/30 mol % DOPC/POPG (noncovalent scheme). The QCM-D Δf and ΔD shifts as a function of time are shown in Figure 5B,C, respectively. A summary of the QCM-D measurement shifts for protein binding at each step is reported in Table 3 below. After C3b attachment that was performed exactly as described above, a mixture of 200 nM factor B and 200 nM factor D was added in order to form the C3bBb convertase. Upon addition of factors B and D, there was a general decrease in the resonance frequency and an increase in dissipation shifts for both SLB platforms. For covalently conjugated C3b on the maleimide-functionalized SLB, the Δf and ΔD shifts were −2.99 ± 0.76 Hz and $(0.39 \pm 0.16) \times 10^{-6}$, respectively. For noncovalently conjugated C3b on the negatively charged SLB, the Δf shift was lower at around −1.44 ± 0.50 Hz, and the ΔD shift was negligible.

Afterward, 500 nM C3 protein was added in order to determine if the assembled C3bBb convertase is enzymatically active at the lipid membrane interface. On the maleimide-functionalized SLB, C3 addition induced a significant decrease in the resonance frequency and an increase in energy dissipation with final values of −26.50 ± 7.91 Hz and $(0.97 \pm 0.22) \times 10^{-6}$, respectively. These measurement responses are attributed to the convertase cleaving the native C3 protein into C3a and C3b fragments, and the generated C3b protein can either be recruited to the C3 convertase (C3bBb) in order to form the C5 convertase or it becomes covalently conjugated to residual free maleimide groups on the SLB surface.[28] In marked contrast, there was essentially no change in the QCM-D measurement signals when C3 was added to the negatively charged SLB, indicating a nonfunctional or incomplete convertase assembly. As a control experiment, C3 protein was also added to covalently attached, membrane-associated C3b protein in the absence of factors B and D, and there was a much smaller Δf shift (less than −5 Hz, an ∼80% decrease) (Figure S6). Collectively, these results support that factor B in the presence of factor D is associated with covalently bound C3, thus creating a functional alternative pathway convertase at the lipid membrane interface. In summary, the results indicate that the covalent immobilization of C3b enables functional

DOI: 10.1021/acs.langmuir.7b01465
Langmuir 2017, 33, 7332−7342

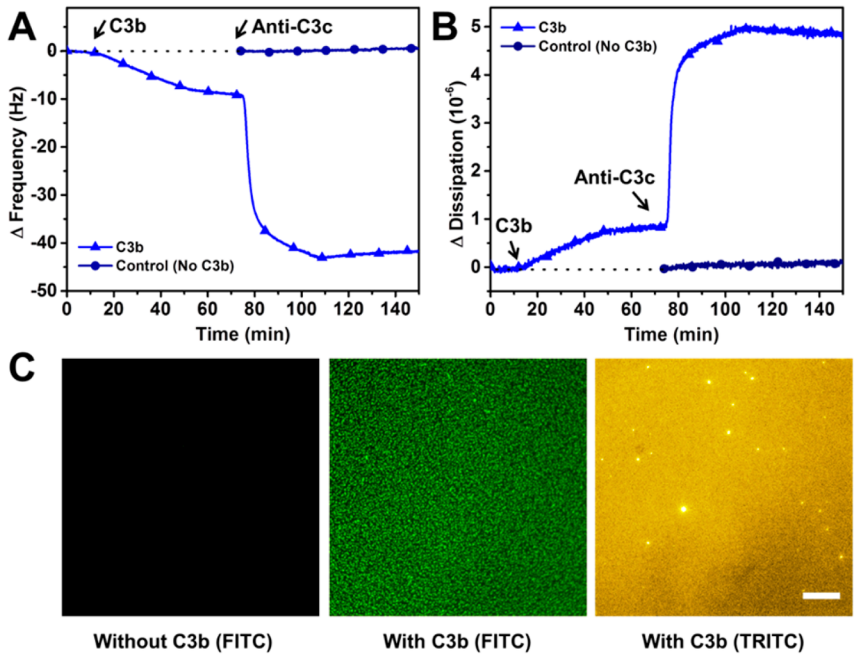

Figure 4. Antibody recognition of membrane-associated C3b protein on a maleimide-functionalized SLB. Changes in QCM-D (A) frequency and (B) energy dissipation as a function of time upon sequential addition of C3b and C3c antibodies (indicated by arrows) onto a maleimide-functionalized SLB with 90/10 mol % DOPC/MPB-PE lipid composition. (C) Fluorescence micrographs of FITC-labeled C3c antibody binding to equivalent SLBs without (left) and with (middle) covalently tethered C3b protein. The TRITC filter set in the left panel reflects the status of SLBs labeled with 0.5 mol % rhodamine−DHPE lipid. The scale bar is 20 μm.

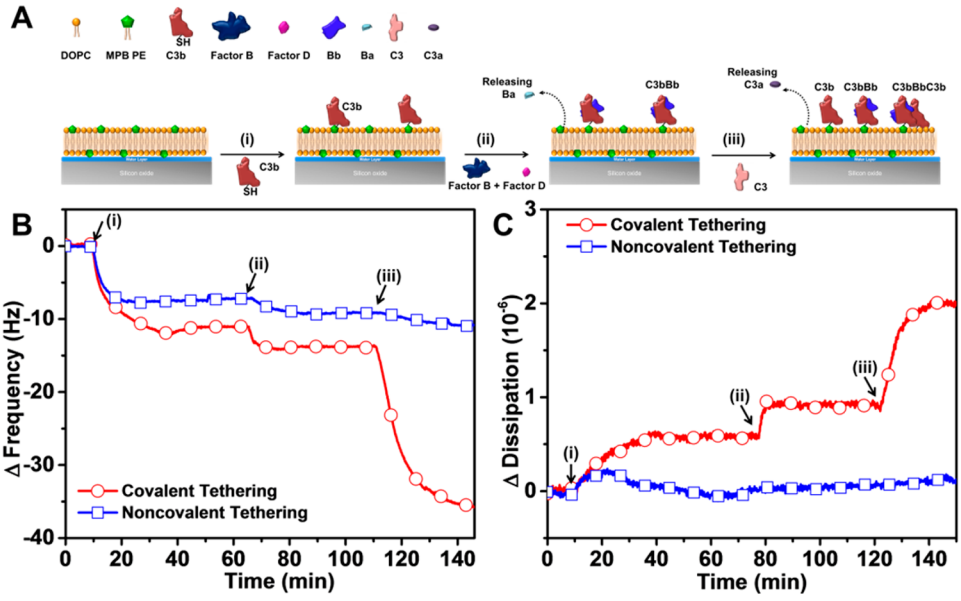

Figure 5. Assembly of alternative pathway C3 convertase on SLB platforms. (A) Schematic illustration of convertase assembly at the lipid membrane interface. (i) C3b protein attachment to SLB. (ii) Addition of complement factors B and D to membrane-associated C3b. In the case of functional C3b, this leads to the formation of C3bBb convertase. (iii) C3 protein addition in order to detect the functional activity of membrane-associated convertase. QCM-D measurements tracked the corresponding changes in (B) frequency and (C) energy dissipation as a function of time.

Table 3. Summary of QCM-D Frequency and Energy Dissipation Shifts for Individual Steps in Convertase Assembly

	covalent tethering		noncovalent tethering	
assembly stage	Δfrequency (Hz)	Δdissipation (10^{-6})	Δfrequency (Hz)	Δdissipation (10^{-6})
(i) C3b	−16.59 ± 4.85	0.89 ± 0.16	−6.36 ± 2.08	0.12 ± 0.09
(ii) factors B and D	−2.99 ± 0.76	0.39 ± 0.16	−1.44 ± 0.50	−0.21 ± 0.07
(iii) C3	−26.50 ± 7.91	0.97 ± 0.22	−1.15 ± 0.21	0.06 ± 0.01

DOI: 10.1021/acs.langmuir.7b01465
Langmuir 2017, 33, 7332−7342

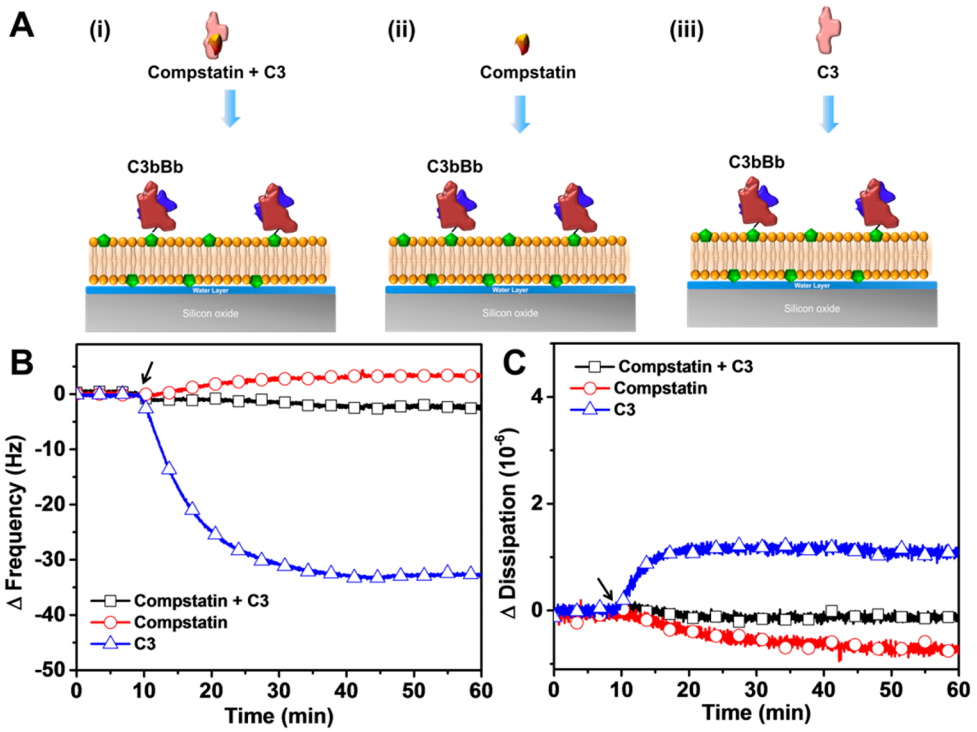

Figure 6. Compstatin-mediated inhibition of C3 cleavage by membrane-associated C3bBb convertase. (A) Schematic illustration of adding (i) a mixture of compstatin and C3, (ii) compstatin alone, or (iii) C3 alone to the membrane-associated, functional C3bB convertase. QCM-D measurements tracked the corresponding changes in (B) frequency and (C) energy dissipation as a function of time.

convertase assembly, whereas the noncovalent scheme led to the formation of an incomplete assembly that was not functional despite a significant amount of bound C3b protein.

Inhibition of C3 Cleavage by Compstatin. To further demonstrate the potential of the SLB platform for evaluating candidate pharmacological inhibitors of convertase function, we investigated the effect of the known complement inhibitor, compstatin (Figure 6A). After establishing the covalently immobilized C3bBb convertase on the SLB platform, the QCM-D measurement responses were normalized to the baseline values, followed by the addition of C3 protein in either the presence or absence of compstatin. When 500 nM C3 protein was added alone to the membrane-associated convertase assembly, convertase-mediated C3 cleavage led to normalized Δf and ΔD shifts of -26.50 ± 7.91 Hz and $(0.97 \pm 0.22) \times 10^{-6}$, respectively (Figure 6B,C; see also Table 3). In contrast, the simultaneous addition of premixed 500 nM C3 and 50 μM compstatin in a 1:100 molar ratio led to normalized Δf and ΔD shifts of -2.80 Hz and -0.06×10^{-6}, respectively, a striking reduction of almost 90% in the measurement responses. As a control, 50 μM compstatin was individually added to the membrane-associated convertase assembly, and the normalized Δf and ΔD shifts were 2.21 Hz and -0.53×10^{-6}, respectively. Taking into account the measurement responses obtained when C3 and compstatin were added together versus when compstatin was added alone, the results support that compstatin caused total inhibition of the convertase function, with the small Δf shift attributed to peptide binding to membrane-associated convertase assemblies. Collectively, the results indicate that compstatin is able to inhibit C3 cleavage by the membrane-associated C3bBb convertase, thereby demonstrating the utility of the SLB platform for evaluating the performance of candidate inhibitors in a biologically relevant membrane environment.

DISCUSSION

Although lipid membranes are ubiquitous biological interfaces, understanding how complement activation occurs at lipid membranes has proven challenging to decipher. Conventional experimental approaches such as ELISA and hemolysis measurements utilize suspended liposomes to determine the extent of complement activation based on the generation of anaphylatoxins or complement complexes or by the release of hemoglobin as discussed above. These measurements take place in a rich biological milieu where the details of the steps by which complement activation occurs are masked, thereby limiting insights into the corresponding molecular mechanisms. Herein, we have utilized a supported lipid bilayer platform in order to reveal the mechanistic factors by which complement activation proceeds at lipid membrane interfaces, namely, the stages of C3 convertase assembly and function. One previous study investigated noncovalent C3 protein adsorption onto zwitterionic lipid bilayers,[59] and this study extends the previous work by demonstrating for the first time the establishment of functional C3 convertases on a supported lipid bilayer, as enabled by a biologically relevant covalent tethering strategy.

C3b protein was chosen to be the complement initiator in our biomimetic design because this protein functions as a positive feedback loop and amplifies complement activation, leading to a rapid and vigorous complement response.[16,60] It is generally understood that the covalent attachment of C3b to a target surface is required in order to trigger complement activation,[12,13] although there are important exceptions. For example, Andersson et al. reported that when C3b proteins are adsorbed noncovalently onto a polystyrene surface the alternative pathway convertase could be successfully formed upon addition of factor B and factor D.[29] Nevertheless, it should be emphasized that early attempts to study convertase

DOI: 10.1021/acs.langmuir.7b01465
Langmuir 2017, 33, 7332−7342

assembly mainly focused on C3b covalent attachment onto SPR sensor chips that require either specific sensor functionalization and/or protein treatment in order to facilitate C3b linkage (e.g., amine-functionalized dextran or streptavidin-coated surfaces and biotinylated C3b).[21,24,25,28] To our knowledge, the role of covalent versus noncovalent attachment schemes was never directly evaluated in previous C3 convertase studies involving any synthetic or natural biomaterial interface.

Importantly, the findings in the present study demonstrate that covalent conjugation of C3b protein via thioether bonds is sufficient to promote convertase assembly on lipid membranes, as achieved using maleimide-functionalized phospholipid headgroups and without requiring protein and surface treatment beforehand. By utilizing this platform, it was observed that C3b protein adsorption was necessary but not sufficient for convertase assembly because only covalently attached protein led to convertase assembly whereas noncovalently attached protein was not successful at supporting functional convertase assembly. Interestingly, only C3b proteins on maleimide-functionalized bilayers facilitated the binding of complement factors B and D, suggesting that covalently bound C3b is required for convertase assembly. Indeed, it has been reported that the covalent attachment of C3b to target surfaces is essential for most downstream complement effector responses,[61,62] and this attachment scheme is considered to be random in orientation because any accessible hydroxyl or amine group on the target surface can, in principle, facilitate C3b covalent attachment.[63] On the basis of the aforementioned CD experimental results, it is likely that more extensive conformational changes, as reflected in the secondary structure analysis, result from covalent immobilization and in turn lead to a greater affinity for C3b binding (e.g., through exposed binding sites).[64] At the same time, even in the absence of functional convertase assembly, noncovalent C3b deposition would likely result in opsonization and stimulate phagocytosis or other relevant immune-mediated clearance mechanisms.

Looking forward in terms of utilizing supported lipid bilayers as model lipid membrane interfaces to host multiprotein enzymatic complexes, there is significant opportunity to explore how lipid membrane properties (e.g., composition, membrane curvature) influence convertase assembly as well as how convertase enzymes at lipid membrane interfaces modulate their specificity or affinity for C3 and C5 proteins, potentially providing insights into the mechanistic regulation of membrane-associated convertase assemblies and conversion processes. Indeed, although a molecular mechanism of alternative pathway C3 convertase assembly has been extensively studied, the molecular details of C5 convertase assembly largely remain to be elucidated. In addition to investigating the macromolecular assembly of convertases, our model system and demonstrated experimental capabilities can also be employed to monitor the dissociation of membrane-bound convertases by complement inhibitors (e.g., complement factor H), which could lead to identifying and validating new therapeutic strategies against many complement-mediated diseases.

CONCLUSIONS

In this study, we have investigated two different tethering strategies in order to form functional complement convertase assemblies at lipid membrane interfaces. Although both covalent and noncovalent immobilization schemes promoted C3b protein attachment to the SLB platform, it was discovered that only covalently attached C3b protein facilitated functional convertase assembly whereas noncovalently attached C3b protein led to incomplete convertase assembly in a nonfunctional state. The QCM-D measurement approach enabled real-time measurement of the protein−protein interactions resulting from convertase assembly as well as the detection of C3 cleavage, which is indicative of functional C3bBb convertases. Importantly, the label-free measurement readout was capable of measuring the compstatin-mediated inhibition of convertase function, thus demonstrating the utility of this measurement platform for candidate inhibitor evaluation. Taken together, the results offer design guidelines for establishing functional biomacromolecular complexes at membrane interfaces and establish a new platform for studying membrane-associated complement convertases in fundamental and translational contexts, including medical device applications.

ASSOCIATED CONTENT

Supporting Information

The Supporting Information is available free of charge on the ACS Publications website at DOI: 10.1021/acs.langmuir.7b01465.

QCM-D and FRAP characterization of supported lipid bilayer formation and control experiments for convertase assembly and antibody binding (PDF)

AUTHOR INFORMATION

Corresponding Author

*E-mail: njcho@ntu.edu.sg.

ORCID

Nam-Joon Cho: 0000-0002-8692-8955

Notes

The authors declare no competing financial interest.

ACKNOWLEDGMENTS

This work was supported by a National Research Foundation grant (no. NRF2015NRF-POC001-019) and an A*STAR-NHG-NTU Skin Research grant (no. SRG/14028) to N.-J.C.

REFERENCES

(1) Carroll, M. C. The complement system in regulation of adaptive immunity. *Nat. Immunol.* **2004**, *5* (10), 981−986.

(2) Ricklin, D.; Hajishengallis, G.; Yang, K.; Lambris, J. D. Complement: a key system for immune surveillance and homeostasis. *Nat. Immunol.* **2010**, *11* (9), 785−797.

(3) Mackay, I. R. Complement. First of two parts. *N. Engl. J. Med.* **2001**, *344* (14), 1058−1066.

(4) Medzhitov, R.; Janeway, C. A. Decoding the patterns of self and nonself by the innate immune system. *Science* **2002**, *296* (5566), 298−300.

(5) Zipfel, P. F.; Mihlan, M.; Skerka, C. The alternative pathway of complement: a pattern recognition system. *Current Topics in Innate Immunity*; Springer, 2007; pp 80−92.

(6) Mollnes, T. E.; Kirschfink, M. Strategies of therapeutic complement inhibition. *Mol. Immunol.* **2006**, *43* (1), 107−121.

(7) Ricklin, D.; Reis, E. S.; Lambris, J. D. Complement in disease: a defence system turning offensive. *Nat. Rev. Nephrol.* **2016**, *12*, 383.

(8) Harboe, M.; Mollnes, T. E. The alternative complement pathway revisited. *J. Cell. Mol. Med.* **2008**, *12* (4), 1074−1084.

(9) Wagner, E.; Frank, M. M. Therapeutic potential of complement modulation. *Nat. Rev. Drug Discovery* **2010**, *9* (1), 43−56.

(10) Sarma, J. V.; Ward, P. A. The complement system. *Cell Tissue Res.* **2011**, *343* (1), 227−235.

DOI: 10.1021/acs.langmuir.7b01465
Langmuir 2017, 33, 7332−7342

(11) Venkatesh, Y. P.; Levine, R. The esterase-like activity of covalently bound human third complement protein. *Mol. Immunol.* **1988**, *25* (9), 821−828.
(12) Law, S.; Dodds, A. W. The internal thioester and the covalent binding properties of the complement proteins C3 and C4. *Protein Sci.* **1997**, *6* (2), 263−274.
(13) Janssen, B. J.; Huizinga, E. G.; Raaijmakers, H. C.; Roos, A.; Daha, M. R.; Nilsson-Ekdahl, K.; Nilsson, B.; Gros, P. Structures of complement component C3 provide insights into the function and evolution of immunity. *Nature* **2005**, *437* (7058), 505−511.
(14) Martin, A.; Lachmann, P.; Halbwachs, L.; Hobart, M. Haemolytic diffusion plate assays for factors B and D of the alternative pathway of complement activation. *Immunochemistry* **1976**, *13* (4), 317−324.
(15) Pangburn, M.; Müller-Eberhard, H. The C3 convertase of the alternative pathway of human complement. Enzymic properties of the bimolecular proteinase. *Biochem. J.* **1986**, *235* (3), 723−730.
(16) Lachmann, P. J. The amplification loop of the complement pathways. *Adv. Immunol.* **2009**, *104*, 115−149.
(17) Alcorlo, M.; Martínez-Barricarte, R.; Fernández, F. J.; Rodríguez-Gallego, C.; Round, A.; Vega, M. C.; Harris, C. L.; et al. Unique structure of iC3b resolved at a resolution of 24 Å by 3D-electron microscopy. *Proc. Natl. Acad. Sci. U. S. A.* **2011**, *108* (32), 13236−13240.
(18) Conrad, D. H.; Carlo, J.; Ruddy, S. Interaction of beta1H globulin with cell-bound C3b: quantitative analysis of binding and influence of alternative pathway components on binding. *J. Exp. Med.* **1978**, *147* (6), 1792−1805.
(19) Pangburn, M. K.; Müller-Eberhard, H. J. Complement C3 convertase: cell surface restriction of β1H control and generation of restriction on neuraminidase-treated cells. *Proc. Natl. Acad. Sci. U. S. A.* **1978**, *75* (5), 2416−2420.
(20) Kazatchkine, M. D.; Fearon, D. T.; Austen, K. F. Human alternative complement pathway: membrane-associated sialic acid regulates the competition between B and β1H for cell-bound C3b. *J. Immunol.* **1979**, *122* (1), 75−81.
(21) Nilsson, B.; Larsson, R.; Hong, J.; Elgue, G.; Ekdahl, K. N.; Sahu, A.; Lambris, J. D. Compstatin inhibits complement and cellular activation in whole blood in two models of extracorporeal circulation. *Mol. Immunol.* **1998**, *35* (6-7), 371.
(22) Harris, C. L.; Abbott, R. J.; Smith, R. A.; Morgan, B. P.; Lea, S. M. Molecular dissection of interactions between components of the alternative pathway of complement and decay accelerating factor (CD55). *J. Biol. Chem.* **2005**, *280* (4), 2569−2578.
(23) Hourcade, D. E. The role of properdin in the assembly of the alternative pathway C3 convertases of complement. *J. Biol. Chem.* **2006**, *281* (4), 2128−2132.
(24) Jokiranta, T. S.; Hellwage, J.; Koistinen, V.; Zipfel, P. F.; Meri, S. Each of the three binding sites on complement factor H interacts with a distinct site on C3b. *Mol. Immunol.* **1998**, *35* (6-7), 360.
(25) Jokiranta, T. S.; Westin, J.; Nilsson, U. R.; Nilsson, B.; Hellwage, J.; Löfås, S.; Gordon, D. L.; Ekdahl, K. N.; Meri, S. Complement C3b interactions studied with surface plasmon resonance technique. *Int. Immunopharmacol.* **2001**, *1* (3), 495−506.
(26) Ricklin, D.; Lambris, J. D. Exploring the complement interaction network using surface plasmon resonance. *Current Topics in Innate Immunity*; Springer, 2007; pp 260−278.
(27) Sarrias, M. R.; Franchini, S.; Canziani, G.; Argyropoulos, E.; Moore, W. T.; Sahu, A.; Lambris, J. D. Kinetic analysis of the interactions of complement receptor 2 (CR2, CD21) with its ligands C3d, iC3b, and the EBV glycoprotein gp350/220. *J. Immunol.* **2001**, *167* (3), 1490−1499.
(28) Berends, E. T.; Gorham, R. D.; Ruyken, M.; Soppe, J. A.; Orhan, H.; Aerts, P. C.; de Haas, C. J.; Gros, P.; Rooijakkers, S. H. Molecular insights into the surface-specific arrangement of complement C5 convertase enzymes. *BMC Biol.* **2015**, *13* (1), 93.
(29) Andersson, J.; Ekdahl, K. N.; Larsson, R.; Nilsson, U. R.; Nilsson, B. C3 adsorbed to a polymer surface can form an initiating alternative pathway convertase. *J. Immunol.* **2002**, *168* (11), 5786−5791.
(30) Hirata, I.; Hioki, Y.; Toda, M.; Kitazawa, T.; Murakami, Y.; Kitano, E.; Kitamura, H.; Ikada, Y.; Iwata, H. Deposition of complement protein C3b on mixed self-assembled monolayers carrying surface hydroxyl and methyl groups studied by surface plasmon resonance. *J. Biomed. Mater. Res.* **2003**, *66* (3), 669−676.
(31) Groves, J. T.; Dustin, M. L. Supported planar bilayers in studies on immune cell adhesion and communication. *J. Immunol. Methods* **2003**, *278* (1), 19−32.
(32) McConnell, H.; Watts, T.; Weis, R.; Brian, A. Supported planar membranes in studies of cell-cell recognition in the immune system. *Biochim. Biophys. Acta, Rev. Biomembr.* **1986**, *864* (1), 95−106.
(33) Yu, C.-h.; Groves, J. T. Engineering supported membranes for cell biology. *Med. Biol. Eng. Comput.* **2010**, *48* (10), 955−963.
(34) Yorulmaz, S.; Tabaei, S. R.; Kim, M.; Seo, J.; Hunziker, W.; Szebeni, J.; Cho, N.-J. Membrane attack complex formation on a supported lipid bilayer: initial steps towards a CARPA predictor nanodevice. *Eur. J. Nanomed.* **2015**, *7* (3), 245−255.
(35) Yorulmaz, S.; Jackman, J. A.; Hunziker, W.; Cho, N.-J. Supported lipid bilayer platform to test inhibitors of the membrane attack complex: Insights into biomacromolecular assembly and regulation. *Biomacromolecules* **2015**, *16* (11), 3594−3602.
(36) Yorulmaz, S.; Jackman, J. A.; Hunziker, W.; Cho, N.-J. Influence of membrane surface charge on adsorption of complement proteins onto supported lipid bilayers. *Colloids Surf., B* **2016**, *148*, 270−277.
(37) Guo, D.; Heitman, L. H.; IJzerman, A. P. Kinetic aspects of the interaction between ligand and G protein-coupled receptor: the case of the adenosine receptors. *Chem. Rev.* **2017**, *117* (1), 38−66.
(38) Inoue, K. The study and application of photoreceptive membrane protein, rhodopsin. *Bull. Chem. Soc. Jpn.* **2016**, *89* (12), 1416−1424.
(39) Shimamoto, K. Elucidation of excitatory neurotransmission and membrane protein integration mechanisms. *Bull. Chem. Soc. Jpn.* **2016**, *89* (3), 282−295.
(40) Janssen, B. J.; Christodoulidou, A.; McCarthy, A.; Lambris, J. D.; Gros, P. Structure of C3b reveals conformational changes that underlie complement activity. *Nature* **2006**, *444* (7116), 213−216.
(41) Janssen, B. J.; Huizinga, E. G.; Raaijmakers, H. C.; Roos, A.; Daha, M. R.; Nilsson-Ekdahl, K.; Nilsson, B.; Gros, P. *Nature* **2005**, *437* (7058), 505−511.
(42) Milder, F. J.; Gomes, L.; Schouten, A.; Janssen, B. J.; Huizinga, E. G.; Romijn, R. A.; Hemrika, W.; Roos, A.; Daha, M. R.; Gros, P. Factor B structure provides insights into activation of the central protease of the complement system. *Nat. Struct. Mol. Biol.* **2007**, *14* (3), 224−228.
(43) Narayana, S. V.; Carson, M.; El-Kabbani, O.; Kilpatrick, J. M.; Moore, D.; Chen, X.; Bugg, C. E.; Volanakis, J. E.; DeLucas, L. J. Structure of Human Factor D: Complement System Protein at 2· 0 Å Resolution. *J. Mol. Biol.* **1994**, *235* (2), 695−708.
(44) Jing, H.; Babu, Y. S.; Moore, D.; Kilpatrick, J. M.; Liu, X.-Y.; Volanakis, J. E.; Narayana, S. V. Structures of native and complexed complement factor D: implications of the atypical His57 conformation and self-inhibitory loop in the regulation of specific serine protease activity. *J. Mol. Biol.* **1998**, *282* (5), 1061−1081.
(45) Sahu, A.; Kay, B. K.; Lambris, J. D. Inhibition of human complement by a C3-binding peptide isolated from a phage-displayed random peptide library. *J. Immunol.* **1996**, *157* (2), 884−891.
(46) Okahata, Y.; Kimura, K.; Ariga, K. Detection of the phase transition of Langmuir-Blodgett films on a quartz-crystal microbalance in an aqueous phase. *J. Am. Chem. Soc.* **1989**, *111* (26), 9190−9194.
(47) Jönsson, P.; Jonsson, M. P.; Tegenfeldt, J. O.; Höök, F. A method improving the accuracy of fluorescence recovery after photobleaching analysis. *Biophys. J.* **2008**, *95* (11), 5334−5348.
(48) Micsonai, A.; Wien, F.; Kernya, L.; Lee, Y.-H.; Goto, Y.; Réfrégiers, M.; Kardos, J. Accurate secondary structure prediction and fold recognition for circular dichroism spectroscopy. *Proc. Natl. Acad. Sci. U. S. A.* **2015**, *112* (24), E3095−E3103.

DOI: 10.1021/acs.langmuir.7b01465
Langmuir 2017, 33, 7332−7342

(49) Tabaei, S. R.; Choi, J.-H.; Haw Zan, G.; Zhdanov, V. P.; Cho, N.-J. Solvent-assisted lipid bilayer formation on silicon dioxide and gold. *Langmuir* **2014**, *30* (34), 10363−10373.
(50) Garcia, B. L.; Summers, B. J.; Lin, Z.; Ramyar, K. X.; Ricklin, D.; Kamath, D. V.; Fu, Z.-Q.; Lambris, J. D.; Geisbrecht, B. V. Diversity in the C3b convertase contact residues and tertiary structures of the staphylococcal complement inhibitor (SCIN) protein family. *J. Biol. Chem.* **2012**, *287* (1), 628−640.
(51) Cho, N.-J.; Frank, C. W.; Kasemo, B.; Höök, F. Quartz crystal microbalance with dissipation monitoring of supported lipid bilayers on various substrates. *Nat. Protoc.* **2010**, *5* (6), 1096−1106.
(52) Thid, D.; Holm, K.; Eriksson, P. S.; Ekeroth, J.; Kasemo, B.; Gold, J. Supported phospholipid bilayers as a platform for neural progenitor cell culture. *J. Biomed. Mater. Res., Part A* **2008**, *84* (4), 940−953.
(53) Svedhem, S.; Dahlborg, D.; Ekeroth, J.; Kelly, J.; Höök, F.; Gold, J. In situ peptide-modified supported lipid bilayers for controlled cell attachment. *Langmuir* **2003**, *19* (17), 6730−6736.
(54) Galush, W. J. *Deconstructing Protein/Protein Signaling Using Supported Lipid Bilayers*; ProQuest, 2008.
(55) Rodahl, M.; Höök, F.; Fredriksson, C.; Keller, C. A.; Krozer, A.; Brzezinski, P.; Voinova, M.; Kasemo, B. Simultaneous frequency and dissipation factor QCM measurements of biomolecular adsorption and cell adhesion. *Faraday Discuss.* **1997**, *107*, 229−246.
(56) Höök, F.; Rodahl, M.; Kasemo, B.; Brzezinski, P. Structural changes in hemoglobin during adsorption to solid surfaces: effects of pH, ionic strength, and ligand binding. *Proc. Natl. Acad. Sci. U. S. A.* **1998**, *95* (21), 12271−12276.
(57) Molenaar, J.; Helder, A.; Müller, M.; Goris-Mulder, M.; Jonker, L.; Brouwer, M.; Pondman, K. Physico-chemical and antigenic properties of human C3. *Immunochemistry* **1975**, *12* (5), 359−364.
(58) Sauerbrey, G. Verwendung von Schwingquarzen zur Wägung dünner Schichten und zur Mikrowägung. *Eur. Phys. J. A* **1959**, *155* (2), 206−222.
(59) Klapper, Y.; Hamad, O. A.; Teramura, Y.; Leneweit, G.; Nienhaus, G. U.; Ricklin, D.; Lambris, J. D.; Ekdahl, K. N.; Nilsson, B. Mediation of a non-proteolytic activation of complement component C3 by phospholipid vesicles. *Biomaterials* **2014**, *35* (11), 3688−3696.
(60) Morgan, B. P.; Harris, C. L. Complement, a target for therapy in inflammatory and degenerative diseases. *Nat. Rev. Drug Discovery* **2015**, *14*, 857−877.
(61) Sim, R.; Twose, T.; Paterson, D.; Sim, E. The covalent-binding reaction of complement component C3. *Biochem. J.* **1981**, *193* (1), 115−127.
(62) Gadjeva, M.; Dodds, A. W.; Taniguchi-Sidle, A.; Willis, A. C.; Isenman, D. E.; Law, S. A. The covalent binding reaction of complement component C3. *J. Immunol.* **1998**, *161* (2), 985−990.
(63) Kim, Y. U.; Carroll, M.; Isenman, D.; Nonaka, M.; Pramoonjago, P.; Takeda, J.; Inoue, K.; Kinoshita, T. Covalent binding of C3b to C4b within the classical complement pathway C5 convertase. Determination of amino acid residues involved in ester linkage formation. *J. Biol. Chem.* **1992**, *267* (6), 4171−4176.
(64) Lewis, L. A.; Ram, S.; Prasad, A.; Gulati, S.; Getzlaff, S.; Blom, A. M.; Vogel, U.; Rice, P. A. Defining targets for complement components C4b and C3b on the pathogenic neisseriae. *Infect. Immun.* **2008**, *76* (1), 339−350.

DOI: 10.1021/acs.langmuir.7b01465
Langmuir 2017, 33, 7332−7342